Characterization of Radio Receiver's Front-End Nonlinearity by Measurement of Spurious-Free Dynamic Ranges

Eugene Sinkevich, Vladimir Mordachev
EMC R&D Laboratory
Belarusian State University of Informatics and Radioelectronics
Minsk, Belarus
emc@bsuir.by

Abstract — **Features and limitations of the radio receiver's front-end nonlinearity characterization technique based on measurements of spurious-free dynamic ranges for intermodulation of different orders are investigated. The technique is familiarly illustrated by the case study (a high-quality radiomonitoring receiver is used as an example): the dynamic ranges for intermodulation of all detected orders (up to 81st) are measured by the instrumentality of the automated double-frequency test system, models of the receiver's front-end nonlinearity are then extracted from the measurement results and validated by experiment.**

Keywords — receiver, intermodulation, dynamic range, behavior simulation, polynomial model

I. INTRODUCTION

Co-site operation of radio equipment (radars, communication, navigation, etc.) is characterized by the presence of powerful out-of-band signals at antenna inputs of radio receivers. These signals can cause a nonlinear interference (intermodulation, desensitization, reciprocal mixing, etc.) in the receivers [1, 2, 3]. Therefore, the prediction of the receivers' nonlinear behavior in the expected electromagnetic environment (EME) is a very important part of co-site electromagnetic compatibility (EMC) analysis.

For behavioral simulation of radio receivers operating in severe EME, the discrete nonlinear analysis (DNA) technology has been developed and successfully applied [4, 5, 6]. This technology has a number of essential features to analyze EMC: 1) simulation in wide frequency and dynamic ranges, 2) account for combined influence of all the fundamental types of nonlinear effects (intermodulation, desensitization, cross-modulation, spurious responses, reciprocal mixing), 3) high computational efficiency (the DNA's computational advantage over traditional techniques grows rapidly with increasing EME complexity and with increasing order of the nonlinear effects).

The use of polynomial models for nonlinearities is a peculiarity of the DNA technology. Such models make it possible to achieve a high dynamic range of nonlinear analysis (up to 300 dB) [4, 5, 6], which gives free scope to analyze intermodulation (IM) and noise-like interference in radio paths.

To synthesize a polynomial model of the receiver's front-end nonlinearity, a technique proposed in [7] may be involved. This technique is of great interest for practice because it does not need detailed initial data for the model extraction: minimum required set of parameters consists of the gain and the spurious-free dynamic range for 3rd-order intermodulation (IDR-3, which is unambiguously related to IP3 [2, 8]). When there are no measurement results, this makes it possible to extract the model of the front-end nonlinearity from the receiver's specification. In the general case, all or several IDRs of orders from 2nd to 25th and/or the spurious-free dynamic range for desensitization (DDR) may be used as initial data for model synthesis.

Let us consider capabilities of a nonlinearity model extracted from IDRs only. By the definition [2, 8], the Kth-order IDR (IDR-K) characterizes only one point of the corresponding intermodulation amplitude response (IMAR-K, which is a dependence of the Kth-order intermodulation component power on the input power per tone). Therefore, in the general case, the model extracted from IDRs only can exactly predict IMAR-K at that point only (even if the model reproduces the IDR-K without error). If the point corresponding to IDR-K belongs to the small-signal region of the IMAR-K (in practice, this holds true only for IMARs of low orders, usually, not above the 9th), then the model is able to exactly reproduce the IMAR-K in the whole small-signal region (in which the influence of nonlinearity of orders $K+2, K+4, \ldots$ on IMAR-K can be neglected, so the slope of IMAR-K in dB/dB is constant and equal to its order K [8]).

That is why the model extracted from IDRs only is recommended to use in the following situations:

1) At early stages of radio systems' design, when the detailed initial data needed for synthesis of more exact model are not available.

2) For EMC analysis of radio systems, when a threshold model is necessary to answer the question "Will the level of intermodulation interference at the receiver output exceed a predefined value called the threshold of susceptibility?" (This threshold value is used in the measurement of IDRs).

In contrast to the traditional technique based on unambiguous conversion of the IDR-*K* to the polynomial coefficient of *K*th-degree term [2, 7, 8], the technique proposed in [7] makes it possible to obtain a physically-adequate (but quantitatively-inaccurate) description for the region of large signal and essential nonlinearity. This is achieved by the use of an intermediate analytical model. The results given in [9] (where the older technique, which is also based on the intermediate analytical model but it does not take into account the IDRs, is utilized) show that the error in the large-signal region of the IMAR-3 is about 10 dB.

Experimental validation of the nonlinear model synthesis technique proposed in [7] is performed in [10], but the influence of the technique's parameters on the quality metrics of resulting models is not studied.

The objective of this paper is to investigate features and limitations of the radio receiver's front-end nonlinearity characterization technique proposed in [7] and based on measurements of different-order IDRs.

The paper is organized as follows. The measurement of IDRs by the instrumentality of the automated double-frequency test system is considered in Section II. The technique for extraction of the receiver's front-end nonlinearity model from measured IDRs is outlined in Section III. In Section IV, models of the front-end nonlinearity are synthesized, and the influence of the technique's parameters (order of the model, maximum order of IDR in the initial data, output threshold used in measurement of IDRs) on the features of the synthesized models is investigated. Validation of the models is given in Section V. In Conclusion, limitations of the model synthesis technique are discussed and recommendations on its improvement are given.

II. Measurement of Intermodulation Dynamic Ranges

The Automated Double-Frequency Test Technique (ADFTT) [11, 12] is a preferable technique to perform the measurement of IDRs. ADFTT makes it possible to easily detect and recognize all interference responses of the receiver under test (RUT) operating in the predicted EME – this helps to choose correct frequency combinations of the input test signals for IDRs measurement. Therefore, the influence of unwanted responses (spurious and intermodulation of non-required types and orders) on measured values of IDRs is eliminated. Modern ADFTT implementations [12] make it possible to measure parameters of RUT nonlinearity of any high order that is necessary for the model synthesis.

The main idea of ADFTT is measurement of a double-frequency diagram (DFD), which is a color map of the RUT's interference responses [12]. A measured DFD of radio receiver is shown in Fig. 1. The RUT is one of the most perfect modern measuring receivers (Schaffner SMR 4518) used in systems of radio monitoring. Measurements are performed with very high levels of the test signals. Note that the test signal levels P_{1in} , P_{2in} are usually selected taking into account the forecast of interfering signal levels at the RUT's input, and sometimes these levels can 20 dB (and more) exceed the threshold of RUT susceptibility to nonlinear effects (IM, desensitization, etc.)

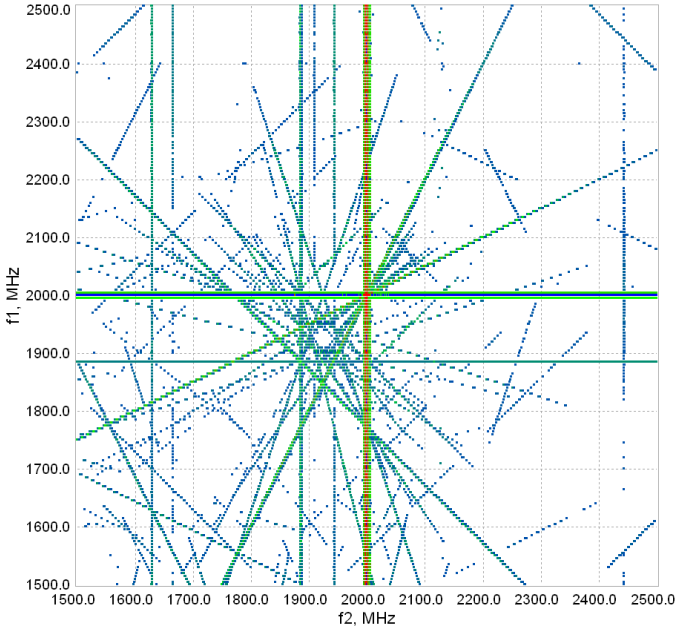

Figure 1. Double-frequency diagram (DFD) of RUT tuned at 2 GHz. Test signal levels $P_{1in} = P_{2in}$ = -5 dBm (105-115 dB above the RUT sensitivity). The display threshold P_t is 3 dB above the internal noise level.

Lines presented in the DFD (ref. Fig. 1) are images of all existing linear and nonlinear signal paths that cause interference at the receiver output: pairs of horizontal and vertical lines crossed on DFD diagonal 45° are images of RUT's desired and spurious responses, inclined lines are images of RUT intermodulation responses.

In Fig. 2, a DFD image obtained for a narrow double-frequency area inside the RUT's preselector passband is given. This area is used for detection and measurement of odd-order intermodulation [11, 12]. DFD given in Fig. 2 contains images of odd intermodulation paths (IMP) of the following type:

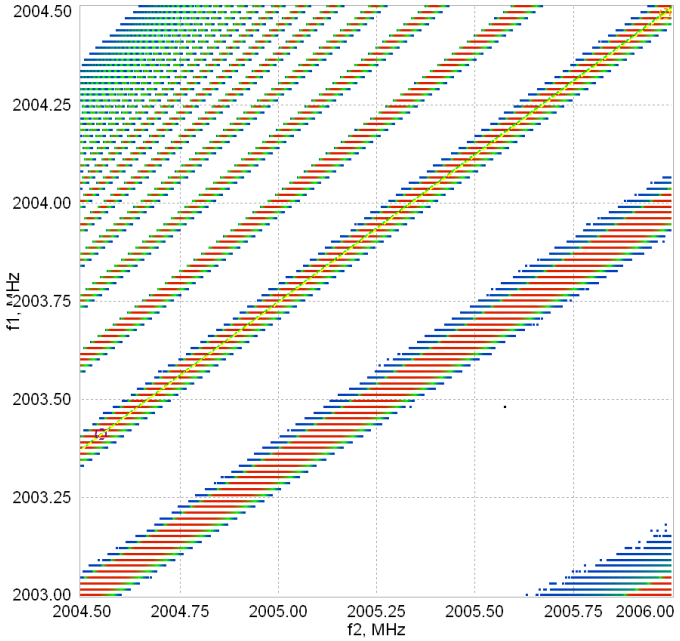

Figure 2. Fragment of the DFD given in Fig. 1: a narrow double-frequency region used for odd-order intermodulation measurement is shown here.

$$(k+1)f_1 - kf_2 = f_{RR}, \quad 2k+1 = K, \quad k = 1, 2 \ldots, \qquad (1)$$

where K is the order of IMP. The image of the 3rd-order IMP is located in the right bottom corner of DFD in Fig. 2, images of IMPs of orders from 5th to 23rd can be identified above the image of the 3rd-order IMP. The images of IMPs of higher orders are difficult to identify in this DFD.

In Fig. 3, a DFD representing the left top fragment of the DFD given in Fig. 2 is shown. In order to obtain this DFD, the frequency sweeping bandwidths were reduced 6 times and the RUT response analysis bandwidth was decreased from 120 kHz to 9 kHz. IMP images of orders from 19th (right bottom corner of the DFD) to 65th are present in this DFD. By setting the display threshold P_t closer to the RUT noise level, the IMP images of orders up to 81st can be detected.

In order to synthesize the front-end nonlinearity model for the RUT, IDRs were measured for all IMPs of type (1) of all orders detected in the DFDs (ref. Figs. 2 and 3). Test signal frequencies for the measurement of IDRs were chosen in the range $[2003; 2006]$ MHz as a result of analysis of the mentioned DFDs. Measurement results are summarized in Table I. The accuracy of the IDR measurement is less than 1 dB, and it is limited by the amplitude setting error of the measurement generators.

The first row in Table I (IM order = 1) corresponds to the measurement of the RUT sensitivity at the tuning frequency of 2 GHz. Output threshold levels P_t = -55 dBm and P_t = -50 dBm are chosen taking into account the noise level at the 3rd intermediate frequency output of the RUT. The noise level measured in the spectrum analyzer's resolution bandwidth of 470 Hz is changed from -70 dBm (for small levels of the test signals) to -61 dBm (for their maximum levels) because of the accompanying reciprocal mixing (this effect is described in [2])

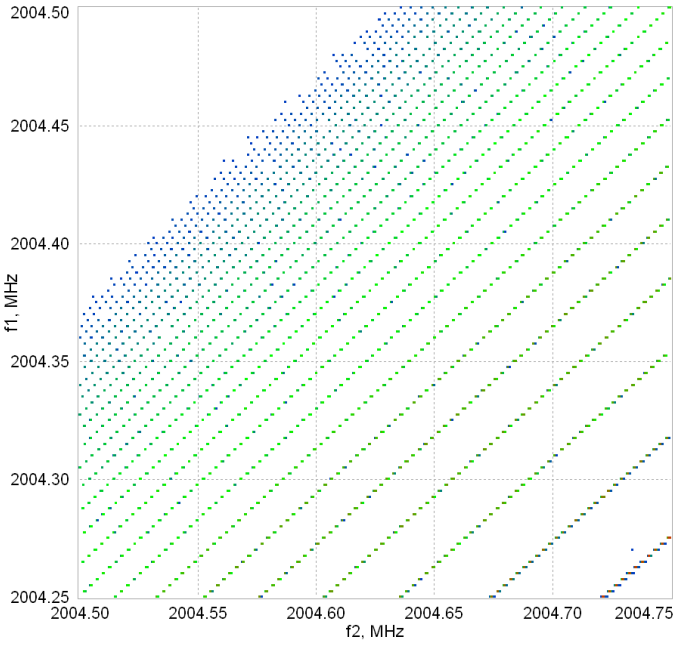

Figure 3. Fragment of the DFD given in Fig. 2: the double-frequency region is reduced here, and the frequency bandwidth of RUT is decreased.

TABLE I. RESULTS OF IDR MEASUREMENTS

IM order (K)	P_t = -55 dBm		P_t = -50 dBm	
	$P_1 = P_2$, dBm	Dynamic Range, dB	$P_1 = P_2$, dBm	Dynamic Range, dB
1	-121.75	0	-116.75	0
3	-38.64	83.11	-36.97	79.78
5	-25.35	96.40	-24.35	92.40
7	-20.62	101.13	-19.38	97.37
9	-16.68	105.07	-16.36	100.39
11	-16.28	105.47	-15.78	100.97
13	-15.82	105.93	-15.42	101.33
15	-14.78	106.97	-14.60	102.15
17	-14.24	107.51	-13.88	102.87
19	-13.58	108.17	-13.34	103.41
21	-13.08	108.67	-12.88	103.87
23	-12.86	108.89	-12.44	104.31
25	-12.58	109.17	-12.12	104.63
27	-12.18	109.57	-11.86	104.89
29	-11.78	109.97	-11.51	105.24
31	-11.40	110.35	-11.10	105.65
33	-11.13	110.62	-10.73	106.02
35	-10.98	110.77	-10.36	106.39
37	-10.66	111.09	-10.00	106.75
39	-10.32	111.43	-9.67	107.08
41	-10.00	111.75	-9.30	107.45
43	-9.74	112.01	-9.04	107.71
45	-9.42	112.33	-8.82	107.93
47	-9.10	112.65	-8.50	108.25
49	-8.78	112.97	-8.18	108.57
51	-8.63	113.12	-7.68	109.07
53	-8.28	113.47	-7.64	109.11
55	-7.94	113.81	-7.38	109.37
57	-7.83	113.92	-7.06	109.69
59	-7.66	114.09	-6.86	109.89
61	-7.28	114.47	-6.54	110.21
63	-6.98	114.77	-6.24	110.51
65	-6.78	114.97	-6.00	110.75
67	-6.52	115.23	-5.82	110.93
69	-6.36	115.39	-5.44	111.31
71	-6.08	115.67	-5.22	111.53
73	-5.82	115.93	-5.04	111.71
75	-5.58	116.17	-4.70	112.05
77	-5.38	116.37	-4.54	112.21
79	-5.14	116.61	-4.30	112.45
81	-4.62	117.13	-4.00	112.75

III. POLYNOMIAL MODEL SYNTHESIS TECHNIQUE

The technique is based on the use of an intermediate theoretical model for the instantaneous transfer characteristic (ITC) [7]. Such model must have a small-signal quasi-linear region and a saturation area. The intermediate models used in this work are listed below. A "Hard limiter" model is described in the normalized form as

$$y(x) = \begin{cases} 1, & 1 < x \le d \\ x & |x| \le 1 \\ -1, & -d \le x < -1 \end{cases}, \quad d = \frac{U_{\max,in}}{U_{s,in}}, \qquad (2)$$

where $x = u_{in} / U_{s,in}$; $y = u_{out} / U_{s,out}$; $U_{s,in}$ and $U_{s,out}$ are saturation voltages with respect to the input and output, correspondingly ($U_{s,out} = G \cdot U_{s,in}$, G is the small-signal gain); $U_{max,in}$ – the maximum voltage at the input.

The other models of type double-sided limiter are "Sine limiter" (3), "Exponential limiter" (4), "Arctangent limiter" (5),

"BJT differential amplifier" (6), "FET differential amplifier" (7), "Error-function limiter" (8) [7, 13]:

$$y(x)=\begin{cases}1, & \pi/2<x<d\\ \sin(x), & |x|\le\pi/2\\ -1, & -d\le x<-\pi/2\end{cases}; \quad (3)$$

$$y(x)=sign(x)\cdot(1-e^{-|x|}),\ |x|\le d; \quad (4)$$

$$y(x)=(2/\pi)\cdot arctg(\pi x/2),\ |x|\le d; \quad (5)$$

$$y(x)=\tanh(x),\ |x|\le d; \quad (6)$$

$$y(x)=\begin{cases}1, & \sqrt{2}<x;\\ x\cdot\sqrt{1-(x^2/4)}, & |x|\le\sqrt{2};\\ -1, & x<-\sqrt{2};\end{cases} \quad (7)$$

$$y(x)=\mathrm{erf}\left(\frac{\sqrt{\pi}}{2}\cdot x\right),\quad \mathrm{erf}(z)=\frac{2}{\sqrt{\pi}}\int_0^z\exp(-t^2)\,dt. \quad (8)$$

The technique is implemented by the following algorithm [7]. At first, a normalized intermediate model is chosen; this model is then approximated in the interval $|x|<d$ by a high-order polynomial using the specially developed interpolation technique. After that, the desensitization dynamic range and the saturation level are found, and the polynomial model is denormalized. Finally, the IDRs are computed for the denormalized model, and a model quality criterion is estimated as RMS error (or as maximum error) between the computed and given IDRs expressed in dB. These steps are repeated for the other polynomial interpolation parameter values and for the other intermediate models, and then the best model (which minimizes the quality criterion) is chosen.

The technique is implemented in "EMC-Analyzer" software [6, 13] which we use for model synthesis in the next Section.

IV. Front-End Nonlinearity Model Synthesis Based on Measured Intermodulation Dynamic Ranges

Based on the measurement results with P_t = -55 dBm (ref. columns 2 and 3 in Table I), a polynomial model of the receiver's front-end nonlinearity was synthesized using the technique from Section III. The following initial data were used for the synthesis: sensitivity MDS = -121.75 dBm, gain $G=P_t/MDS=66.75$ dB, order of the model $M=25$, spurious-free dynamic ranges for intermodulation (IDRs) of odd orders (from 3rd to 25th). The best model was found by minimization of the criterion "RMS error in IDR" (minimization of the criterion "Max. error in IDR" yields similar results for the considered initial data). Approximation range (d) optimization was additionally performed: for large values of d, the error of IDRs approximation is increased; for small values of d, the peak input signal is decreased (Table II). The results of model synthesis with optimal value $d_0=1.9$ are given in Table III and in column "1" of Table IV (each error is a difference between the value simulated by the model and the measured value); the instantaneous transfer characteristic (ITC) for voltage is plotted in Fig. 4 (line m1). The ITC behavior in the input signal range of (149; 210) mV should be considered as extrapolation because the maximum (peak) input voltage used in the measurement of IDRs is of 149 mV (-12.58 dBm/tone @ 50 Ohm load); the behavior of polynomial is physically inconsistent if the input signal exceeds the approximation range bound of 210 mV.

ITCs plotted in Fig. 4 characterize the nonlinearity of the receiver's front-end: saturation level wrt output (over 200 V) is obtained for ideal (perfectly linear) output circuit. Note that the measured saturation level of the amplitude-to-amplitude characteristic for the whole receiving path (from the receiver input to the 3rd intermediate frequency output) is caused by the output nonlinearity – this level is only 123 mV (-8.2 dBm @ 50 Ohm load), therefore, the ITC's saturation level for the whole receiver is of $123\cdot\pi/4=96.6$ mV.

TABLE II. Approximation Range Optimization

Parameter	Value					
Appoximation range (d)	1.1	1.5	1.9	2.7	3.5	5.5
RMS error in IDRs, dB	1.24	1.37	1.30	1.55	2.40	3.44
Peak input signal, mV	80	202	210	204	245	280

TABLE III. Extracted Model 1

Order (*K*)	Polynomial coefficient, $V^{(1-K)}$	Error in IDR, dB	Error in IM level, dB [a]	
1	2.17521433088214E+03	—	—	
3	-2.62364608886398E+04	-1.65	4.95	(4.95)
5	7.46792717276267E+05	-0.74	3.67	(3.70)
7	2.93327898802524E+08	-1.34	10.88	(9.38)
9	-1.69032767897740E+11	-2.16	23.26	(19.44)
11	3.05319618082546E+13	-0.24	6.25	(2.64)
13	-2.92152320564768E+15	-0.82	3.20	(10.66)
15	1.69285631537154E+17	1.54	5.66	(-23.10)
17	-6.25331912820014E+18	-0.13	1.47	(2.21)
19	1.48669578130813E+20	0.27	-3.79	(-5.13)
21	-2.20861692710256E+21	0.77	-12.99	(-16.17)
23	1.86982441322147E+22	1.49	-30.51	(-34.27)
25	-6.89955690129789E+22	2.12	-52.90	(-53.00)

a. Small-signal estimations are given in parentheses

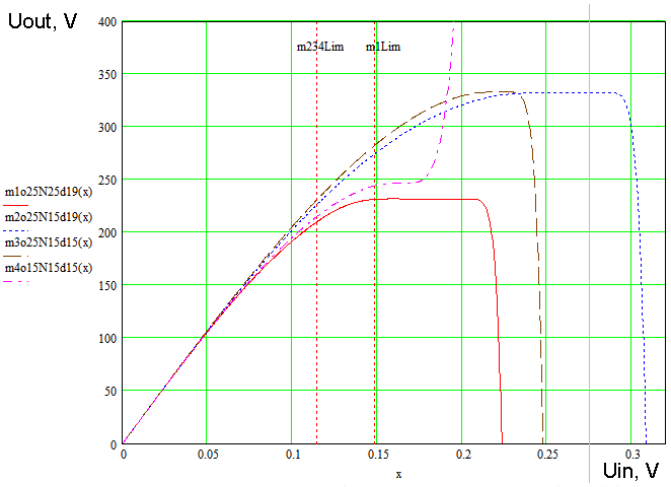

Figure 4. Instantaneous transfer characteristics of extracted models (one side of odd functions is shown).

TABLE IV. PARAMETERS OF EXTRACTED MODELS

Parameter	Model			
	1	*2*	*3*	*4*
Polynomial order (M)	25	25	25	15
Max. given IDR order (N)	25	15	15	15
Appoximation range (d)	1.9	1.9	1.5	1.5
Intermediate model	(7)	(3)	(7)	(7)
Saturation wrt input, mV	108	153	154	114
RMS error in IDRs, dB [a]	1.30	1.12	1.03	1.12
Max. error in IDRs, dB [a]	2.16	2.00	2.04	1.82
Error in IDR3, dB	-1.65	0.15	0.89	-0.87
Error in IDR5, dB	-0.74	0.01	0.94	0.00
Peak input signal, mV:				
in data (Table I) [b]	149	115	115	115
for model (Fig. 4)	210	290	231	175
Level prediction error, dB:				
2-signal IM3 at 2 GHz	4.95	-0.44	-2.68	2.61
3-signal IM3 at 2 GHz	4.85	-0.52	-2.76	2.52

a. IDRs of odd orders from 3rd to Nth were considered

b. Power per tone (given for Nth-order IDR) was recomputed into peak voltage at 50 Ohm load

In order to investigate the influence of the polynomial model's order M and the maximum order of IDR in the initial data N on the characteristics of the resulting models, another models were extracted from the truncated initial data (IDRs of odd orders from 3rd to 15th were used). 25th-order models were considered at first, and then we examined 15th-order models. Approximation range (d) optimization yields 2 models of 25th order (models "2" and "3") and one 15th-order model (labeled as "4"). Parameters of those models are given in columns "2", "3", and "4" of Table IV, and the corresponding ITCs are plotted in Fig. 4 (lines m2, m3, and m4). The models have the following differences from the model "1":

1) The difference between the computed and given (measured) IDRs is changed: the distinction is decreased for IDRs of orders 3, 5 ... 15 (ref. lines "RMS error in IDRs", "Error in IDR3", and "Error in IDR5" in Table IV), and it is increased for IDRs of orders 17, 19 ... 25 (since these IDRs were not used for model synthesis). Model "4" does not reproduce an intermodulation (IM) of order higher than 15th.

2) The model adequacy range restricted by initial data is decreased from 149 mV to 115 mV (in compliance with the 15th-order IM susceptibility level: -17.78 dBm/tone @ 50 Ohm load).

3) The rest of the characteristics (intermediate theoretical model type; saturation level wrt input; peak input voltage for model, which is limited by physically-consistent behavior of the polynomial) may vary depending on model, which is illustrated in Table IV.

After that, the influence of the threshold P_t on the model synthesis results was investigated. For this purpose, the 25th- and 15th-order models were extracted from the second set of initial data (i.e., from the results of measurements with P_t = -50 dBm – ref. columns 4 and 5 in Table I); both full and truncated data were used as before. Each of the models almost coincides with the analogous model extracted from the first data set (measured with P_t = -55 dBm), including the following: optimal values of the parameter d, ITC plots, and differences between the given and computed IDRs.

V. VALIDATION OF THE SYNTESIZED MODELS

In order to validate the synthesized models of the receiver's front-end nonlinearity, the levels of IM components at the 3rd intermediate frequency output were computed by the models and compared to the measured ones. The validation was performed in three stages:

1) The measurement of IDR3 was simulated to check if the level of two-signal 3rd-order intermodulation (IM3) is reproduced correctly. For this purpose, a two-tone signal with the following parameters of the components was fed to the nonlinearity model input: frequencies were f1 = 2003 MHz, f2 = 2006 MHz, amplitudes Um1 = Um2 = 3.70 mV were equal to the measured susceptibility level for IM3 (-38.64 dBm/tone @ 50 Ohm load – ref. Table I). The level estimation error for IM3 arisen at frequency $f_{2,-1} = 2 \cdot f_1 - f_2 = 2000$ MHz (a ratio of the level computed by the model to the measured value of $P_t = -55$ dBm) is given in row "2-signal IM3 at 2 GHz" of Table IV for each model.

The mentioned error depends on the IDR3 approximation error (ref. Table IV), because the slope of amplitude characteristic for *K*-th-order intermodulation (AC-IM-*K*) is equal to *K* (dB/dB) in small-signal mode (ref. Introduction): e.g., the IDR3 approximation error for nonlinearity model "1" is of –1.65 dB, therefore, the error in IM3 level is equal to $-3 \cdot (-1.65) = 4.95$ dB .

2) For the model "1", the measurements of high-order IDRs were simulated in the same way as for IDR3. The errors in levels of the IM components were found by simulation and estimated under the small-signal assumption. Let us analyze the obtained results (ref. the last column in Table III): IDRs of orders 3…7 describe the small-signal mode, in which the slope of AC-IM (dB/dB) is equal to its order; beginning from the 9th order (in principle, this order depends on the output threshold – in our case $P_t = -55$ dBm), a strong influence of the higher-order nonlinearity is observed (the slope of ACs-IM is changed); then, beginning from the 21st order, this influence is relaxed again because the order of nonlinearity is limited by the order of the polynomial model.

3) Additional measurements were performed to check the simulation of a three-signal IM3 level: a three-tone signal having the component frequencies f1 = 1997 MHz, f2 = 2003.5 MHz, f3 = 2006.5 MHz and powers P1 = - 40.58 dBm, P2 = P3 = - 40.37 dBm was fed to the receiver input. The level of a three-signal IM3 arisen in the receiver's front-end at the tuning frequency $f_{1,-1,1} = f_1 - f_2 + f_3 = f_1 + \Delta f_{32} = 2000$ MHz , $\Delta f_{32} = f_3 - f_2$, was measured at the 3rd intermediate frequency output – the measurement result is -54.3 dBm. The error in estimation of the mentioned component level was computed for each model – ref. row "3-signal IM3 at 2 GHz" in Table IV. An output spectrum of the recever's front-end nonlinearity model "1" fed by the above-mentioned three-tone input stimulus is given in Fig. 5 (the frequency filtering is not accounted for).

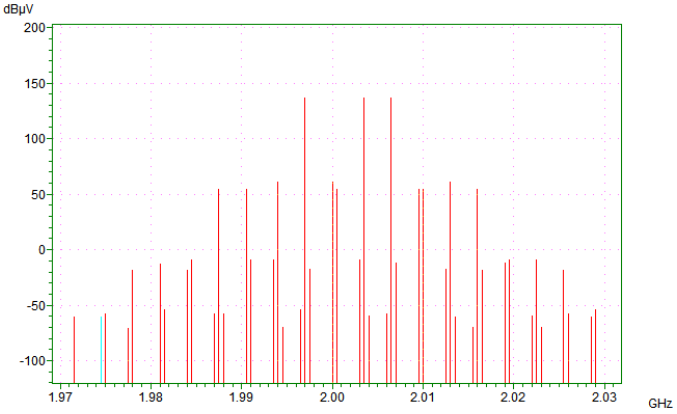

Figure 5. Simulated spectrum at the nonlinearity output for 3-tone input signal (note the level differences between components of orders 1, 3, 5, 7). Dynamic range of simulation is 220 dB.

VI. CONCLUSION

1) Model "2" should be recognized as the best among the synthesized models (ref. Table IV) because it reproduces the IDRs and levels of low-order (3rd and 5th) IM components more accurately. The low-order components are the most dangerous since they have higher levels than the other components – ref. Fig. 5.

Since the criterion "RMS error in IDRs" has not shown the optimality of the model "2" (ref. Table IV), it is necessary to improve this criterion: the errors in IDRs of lower orders must have larger weights. In addition, it is desirable to automate the approximation range (d) optimization (ref. Table II) and the polynomial order (M) optimization (ref. Table IV).

2) If the synthesized model is used for prediction of intermodulation levels (i.e., not as a threshold model – ref. Section I), it is important to keep in mind that low errors in prediction of IDRs may cause large errors in IM levels (ref. Table III and Section V). A little margin in order of the model (e.g., $M = N + 6$ in designations of Table IV) makes it possible to avoid the large errors in levels of highest-order $(N, N-2, N-4)$ IM components.

Note that the errors in approximation of measured IDRs by the model can in principle be reduced by improving the synthesis technique (e.g., by increasing the number of the intermediate models – ref. Section III), as opposed to the IDR measurement errors that depend on the employed equipment (e.g., the level accuracy of modern signal generators is usually about 0.5…1 dB [14]).

3) The nonlinearity models extracted from IDRs only predict the saturation region not in the best way (ref. Fig. 4). To improve this, one needs to measure the dynamic range for desensitization and include it into the initial data for the model synthesis (the technique has such option [7, 10, 13]).

REFERENCES

[1] A handbook series on electromagnetic interference and compatibility, Vol.7: Duff W.G. Electromagnetic compatibility in telecommunications. Interference Control Technologies, Inc., Gainesville, VA, 1988.

[2] Rohde U.L., Whitaker J. Communications Receivers: DSP, Software Radios, and Design, 3rd Edition, McGraw-Hill, New York, 2000.

[3] Lustgarten M.N. Significant receiver intermodulation (RIM) products // IEEE Symp. on EMC, 1979, pp. 314–318.

[4] Mordachev V.I. Express analysis of electromagnetic compatibility of radio electronic equipment with the use of discrete models of interference and fast Fourier transform // IX Int. Wroclaw Symp. EMC, 1988, pp. 565–570 (in Russian).

[5] Loyka S.L., Mosig J.R. New behavioral-level simulation technique for RF / Microwave applications. Part I: Basic concepts // Intern. J. RF and Microwave CAE. 2000. Vol. 10, No. 4, pp. 221–237.

[6] Mordachev V.I., Sinkevich E.V. "EMC-Analyzer" expert system: improvement of IEMCAP models // XIX Int. Wroclaw Symp. EMC. 2008, pp. 423–428.

[7] Cheremisinov I.D., Loyka S.L., Mordachev V.I. Synthesis of the polynomial model of nonlinear elements based on intermodulation dynamic ranges // 3rd Int. Conf. on Telecommunications in Modern Satellite, Cable, and Broadcasting Services (TELSIKS'97), Oct. 8-10, 1997, Nis, Yugoslavia, pp. 519–522.

[8] Pedro J.C., Carvalho N.B. Intermodulation Distortion in Microwave and Wireless Circuits, Artech House, Boston, 2003.

[9] Cheremisinov I.D., Loyka S.L. Polynomial models of radio system nonlinear stages for the discrete EMC analysis // 8th Int. Crimean Conf. Microwave & Telecommunications Technology (CriMiCo 98). Crimea, Ukraine, Sep. 14–17, 1998, pp. 408–409.

[10] Cheremisinov I.D. Selection of polynomial model based on intermodulation dynamic ranges // 4th Int. Conf. on New Information Technologies (NITe'2000), Dec. 5-7, 2000, Minsk, Belarus, pp. 133–140 (in Russian).

[11] Mordachev V.I. "Automated double-frequency testing technique for mapping receiver interference responses" // IEEE Trans. on EMC, vol.42, No.2, pp. 213–225, May 2000.

[12] Mordachev V.I., Sinkevich E.V. Experimental Analysis of Radio Receiver Susceptibility to Out-of-Band Interference by Means of Double-Frequency Test System // Proceedings of the 10-th Int. Symp. on EMC "EMC Europe 2011", UK, York, Sept. 26-30, 2011, pp. 405–411.

[13] EMC-Analyzer. Mathematical models and algorithms of electromagnetic compatibility analysis and prediction software complex. Minsk, 2011.

[14] Data Sheets of Signal Generators E4438C, E8267D, N5182A. Available: http://www.agilent.com